nature neuroscience

Optimal sensorimotor transformations for balance

Daniel B Lockhart[1] & Lena H Ting[2]

Here we have identified a sensorimotor transformation that is used by a mammalian nervous system to produce a multijoint motor behavior. Using a simple biomechanical model, a delayed-feedback rule based on an optimal tradeoff between postural error and neural effort explained patterns of muscle activation in response to a sudden loss of balance in cats. Following the loss of large sensory afferents, changes in these muscle-activation patterns reflected an optimal reweighting of sensory feedback gains to minimize postural instability. Specifically, a loss of center-of-mass-acceleration information, which allowed for a rapid initial rise in the muscle activity in intact animals, was absent after large-fiber sensory neuropathy. Our results demonstrate that a simple and flexible neural feedback control strategy coordinates multiple muscles over time via a small set of extrinsic, task-level variables during complex multijoint natural movements.

The simple act of standing up is a common and essential motor behavior that is often taken for granted, even in uncertain and dynamic environments. Although humans are able to stand on a boat or walk over uneven terrain without much thought, the neural systems that regulate postural orientation and equilibrium continually integrate a large array of sensory inputs and coordinate multiple motor outputs to muscles throughout the body. Understanding how complex sensory patterns are transformed into an appropriate temporal sequence of motor commands is central to unraveling the complexities of the neural control of movement.

It has been shown recently that just a few motor command signals are used to generate spatial patterns of muscle activation during natural movements[1–4]. By using a single motor command signal to activate multiple muscles across the body in a group, called a 'muscle synergy', a multijoint motion can be produced. By adding a few additional motor command signals, a repertoire of complex motions becomes possible. The advantage of this scheme is that the set of motor command signals has substantially reduced dimension when compared with the total number of motor outputs[5], whether these are considered to be individual muscles or motor units. During a natural movement, these motor command signals are necessarily modulated over time[6,7]; however, the neural mechanisms that determine their temporal characteristics are not known.

In balance control in particular, motor command signals must be dynamically modulated in response to a suite of sensory information and cannot be generated by feedforward spinal pattern-generation mechanisms, such as those producing locomotion[3,8]. Sensory signals during a perturbation also depend dynamically on the ongoing motor response to the perturbation, making them difficult to study in a classical stimulus-response procedure. Moreover, because of redundancy in the multijointed musculoskeletal system, the relationships between specific joint-angle changes and muscle-activation patterns during the postural response are highly variable[9]. Thus, postural responses to perturbations cannot be explained by reflex loops acting on individual joint angles, but instead require substantial integration of multiple sensory modalities, presumably in the brainstem[10].

Because the center of mass (CoM) motion compactly encapsulates the relationship of the body to the extrinsic effects of gravity and external forces, we reasoned that the control of CoM dynamics would be important in the feedback regulation of balance. The best predictor of which muscles are activated during a postural response to perturbation is the horizontal direction of CoM motion[9,11]. CoM-motion variables are extrinsic, task-level variables that represent the net motion of the body with respect to the gravitational reference frame. In general, extrinsic, task-level variables represent the relative relationship of multiple body segments to the external environment and cannot be inferred from local anatomical variables such as joint angles or head displacement, except in the simplest of cases. Thus, task-level variables generally cannot be encoded by any one sensory signal or modality; rather, they must be estimated from many sensory modalities.

We hypothesized that an optimal and hierarchal feedback control organization based on extrinsic, task-level variables governs balance control, which is an automatic motor task that does not require trajectory planning or the involvement of higher brain centers[10]. Similar schemes have been proposed as a general organization principle for voluntary motor tasks[12–16]. We predicted that neural control mechanisms for temporal patterning of motor signals for balance control would be low in dimension, operating on a small set of feedback gains related to the control of the CoM[5]. We demonstrate that a simple model of the neuromechanical system—an inverted pendulum stabilized by a feedback rule—predicts the time course of motor command signals during balance control in both intact and sensory-loss cats. The pendulum dynamics nominally modeled CoM acceleration, velocity and position of the animal and were sufficient to specify the motor

[1]Woodruff School of Mechanical Engineering, Georgia Institute of Technology and [2]Coulter Department of Biomedical Engineering, Emory University and Georgia Institute of Technology, 313 Ferst Drive, Atlanta, Georgia 30332-0535, USA. Correspondence should be addressed to L.H.T. (lting@emory.edu).

Received 5 July; accepted 24 August; published online 16 September 2007; doi:10.1038/nn1986

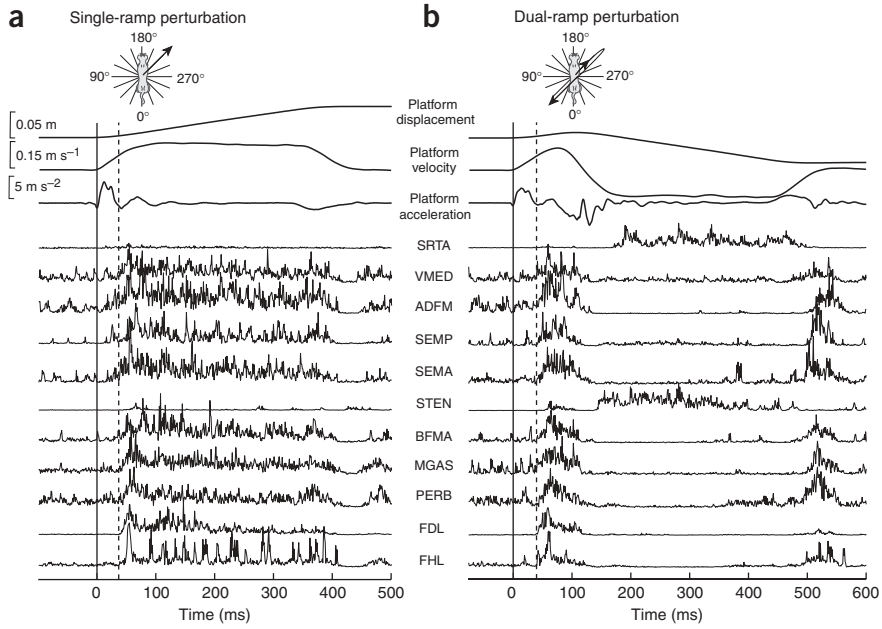

Figure 1 Example of muscle-activation patterns evoked during balance corrections to support-surface motion in the horizontal plane. Cats were freely standing on a movable platform that could move in the horizontal plane. EMGs were measured in the left hindlimb. (**a**) Responses to a ramp-and-hold perturbation in the 225° direction evoked a classic EMG pattern of an initial burst followed by a long plateau in multiple extensor muscles, whereas the flexor muscles (STEN) were quiescent. The initial burst shape followed the perturbation acceleration after a short delay of about 30 ms. The duration of the plateau followed the velocity of the perturbations. (**b**) Responses to a dual-ramp perturbation in which the direction of support-surface motion is reversed 20–90 ms after onset of the initial ramp. These perturbations allowed us to test the robustness of the feedback model by altering the acceleration waveform associated with the initial ramp, as well as the CoM velocity and position at the onset of the secondary ramp. Because muscle activity is direction-specific, the extensor muscles originally activated by the perturbation were shut off, and flexor muscles were activated. Muscle abbreviations: biceps femoris anterior, BFMA; flexor digitorum longus, FDL; flexor hallicus longus, FHL; medial gastrocnemius, MGAS; peroneous brevis, PERB; semimembranosus anterior, SEMA; semimembranosus posterior, SEMP; sartorius anterior, SRTA; semitendinosus, STEN; vastus medialis, VMED.

command signals activating both proximal and distal leg muscles. To our surprise, the resulting patterns of muscle activation were also similar to the optimal patterns predicted using an objective criterion drawn from optimal control theory. Moreover, the predictions were robust to peripheral sensory neuropathy, which disrupts the encoding of local joint-angle changes by large-diameter sensory afferents[17]. Following re-adaptation subsequent to this acute sensory deficit, temporal motor patterns were markedly altered, but in the model resulted simply from a loss of CoM acceleration feedback. Our approach of defining temporal patterns of muscle activity in normal and neurologically impaired animals with a neuromechanical model using feedback of extrinsic, task-level variables provides new insight into the robust structure of general sensorimotor transformations for movement control.

RESULTS

Simple feedback transformation for postural control

We examined temporal patterns of muscle activation that were evoked by translation of the support surface in unrestrained, freely standing cats. The perturbations elicited a maximal response in the left hindlimb muscles and minimal responses in the other limbs[18]. The temporal responses in the majority of the extensors were similar, suggesting that common neural signals modulated multiple muscles (**Fig. 1**). The response to single-ramp perturbations was also similar to that observed in humans[10,19]: an initial burst followed by a long plateau of activity (**Fig. 1a**). The initial burst of the elicited responses had a shape similar to that of the temporal pattern of support-surface acceleration, but with a latency of 30–50 ms. The durations of the muscular response and perturbation were also similar. However, the animal's sensory system cannot directly encode the motion of the support surface, only the effects of that motion on the animal's own body. The time lags between CoM kinematics and muscle-activation patterns led us to hypothesize that the nervous system uses an estimate of overall body movement in a feedback manner to regulate temporal patterns of muscle activation.

To functionally and quantitatively test this hypothesis, we developed a simple computational model of postural control (**Fig. 2**) and evaluated how well it explained muscle-activation patterns that we observed experimentally. We parameterized the model first on the basis of experimental data, and second to maximize an objective-cost function based on performance measures. The model consisted of an inverted pendulum actuated at the base by a muscle and mounted on a moveable support surface (**Fig. 2a**). The experimentally recorded acceleration of the support surface was used as the only input to the model. The hypothesized neural controller constructed temporal patterns of muscle activation from linear combinations of the simulated CoM position, velocity and acceleration signals[12,14] (**Fig. 2b**), delayed in time to account for latencies due to neural conduction and computation, and assumed to be estimated by the nervous system from an ensemble of sensory signals[10,20,21]. An advantage of this forward modeling approach is that the biomechanical viability of the sensorimotor transformation is implicitly tested; solutions derived from measured kinematic signals do not generally stabilize the system[22].

Identification of model parameters

Variations of only four parameters in our model, three feedback gains and one delay, were sufficient to reproduce salient features in each of the experimentally measured muscle-activation patterns (see Methods; variability accounted for (VAF) = 88 ± 2% s.e.m. across cats, VAF > 80% for all muscles across all cats). For each muscle in each animal, we identified three feedback gains and one delay that best matched the muscle activation and kinematics of the simulation to experimental data. We dubbed this process temporal system identification (TSyID) because model parameters were found by matching features of the data in the temporal domain. Although we nominally modeled only the net motion of the CoM, and not individual joints, muscles crossing all joints were analyzed to test whether CoM kinematics were sufficient to reproduce all muscle-activation patterns.

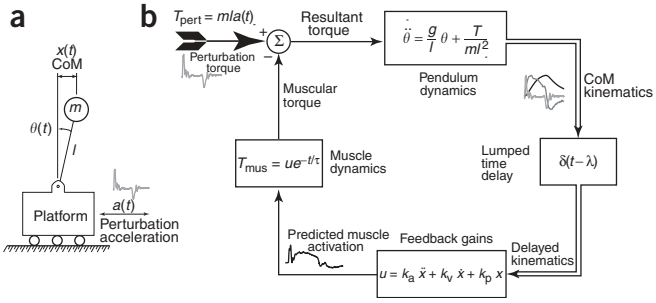

Figure 2 Simple feedback model of postural control used to predict muscle activity during balance responses. (**a**) The mechanics of the CoM during the balance task is approximated as an inverted pendulum on a moving cart. Experimentally measured accelerations of the platform were applied to the cart so that realistic acceleration, velocity and displacement trajectories of the platform were modeled. (**b**) The perturbation acceleration generates a disturbance torque at the base of the pendulum. Delayed kinematics of the horizontal CoM were used in a simple feedback law to generated model muscle-activation patterns, which were compared with those measured experimentally. The model muscle activation then generated a stabilizing torque about the representative joint.

The initial burst and plateau in the muscle-activation patterns were well reproduced (**Fig. 3**) by the model. CoM position, acceleration and velocity were also similar in experiments and simulations (**Fig. 3a**). The initial burst of muscle activity (**Fig. 3b**) was generated by the CoM acceleration signal, rather than by a predictive feedforward signal as previously suggested[19], whereas the plateau was a result of velocity and position feedback (**Fig. 3c**). Because of the physical dynamics of the signals, acceleration information was available before velocity increased appreciably. In turn, the position signal took the longest to evolve and was only influential toward the end of the temporal pattern of muscle activation. Although each feedback channel was subject to the same lumped time delay, the mechanical dynamics of the system accounted for the different time course of each feedback signal. The predictive power was not improved by altering the number of parameters in the model. When we eliminated acceleration feedback, the initial burst was not predicted, and the model fits to data decreased modestly, but consistently (paired *t*-test, $\Delta VAF = -2\%$, $P < 0.01$). When a CoM-jerk-feedback term or multiple delay terms were added, model fits to data did not improve ($P > 0.05$).

In each animal, the temporal pattern of activation in each muscle reflected a slightly different combination of CoM kinematic variables (**Fig. 3d**). However, we found significant differences in acceleration- ($P < 0.01$) and position-feedback gains ($P < 0.01$) across animals, suggesting that each animal used a characteristic combination of feedback gains (**Fig. 4**). The consistency in the feedback gains in each animal supports the idea that proximal and distal muscle-activation patterns are coupled via muscle synergies that activate multiple muscles across the limb with differential weighting[1–3,23,24]. This coupling of distributed muscles may be necessary to produce coordinated actions across joints during balance control[25,26].

We also collected postural responses to dual-ramp perturbations that substantially altered the temporal patterns of perturbation acceleration, velocity and position by reversing platform direction after 20–90 ms (**Fig. 1b**). Experimentally, this resulted in changes in both the initial CoM-acceleration patterns and the CoM kinematics when the longer secondary perturbation, which was identical to the single-ramp perturbations, was presented. Accordingly, as extensor muscles were highly active in the 225° direction (**Figs. 1a** and **5a**), but quiescent in the 45° direction (**Fig. 5b**), extensor muscles were either activated for a short period of time in response to an initial 225° ramp (**Figs. 1b** and **5c**) or activated later for a longer duration in response to a secondary 225° ramp (**Fig. 5d**).

We cross-validated the predictive power of our model by simulating responses to dual-ramp perturbations (**Fig. 5c**,**d**) without altering the feedback parameters derived from the single-ramp perturbations (**Fig. 5a**,**b**). The model predicted changes in the initial extensor bursts in response to short 225° perturbations (for example, **Fig. 5c**; VAF = 86 ± 8%), which were due primarily to changes in initial perturbation acceleration. The timing of the small burst at the end of the secondary ramp was also predicted by the model (**Fig. 5c**). Extensor responses to the longer secondary perturbations were also qualitatively well accounted for (**Fig. 5d**), particularly the timing of the onset and offset

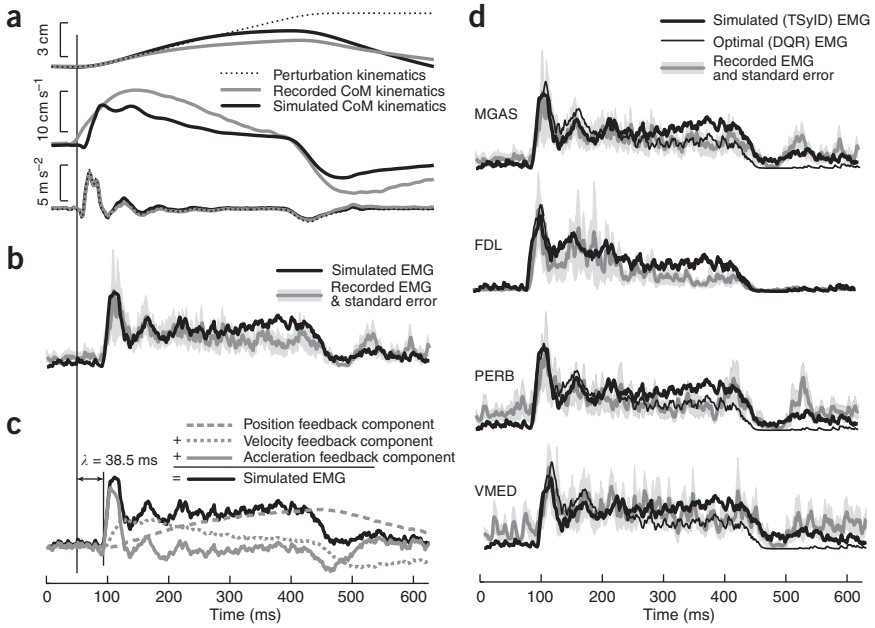

Figure 3 Comparison of recorded and simulated muscle activation and CoM kinematics. (**a**) Recorded (gray lines) and simulated (black lines) CoM displacement, velocity and acceleration. (**b**) Recorded (gray line) muscle activity in the MGAS and simulated (black line) muscle activity from the best-match model parameters derived from the TSyID formulation of the model. (**c**) Decomposition of simulated muscle activity (black line) into components arising from CoM position feedback (gray dashed line), CoM velocity feedback (gray dotted line) and CoM acceleration feedback (gray solid line). Note that the initial burst is due primarily to acceleration feedback. (**d**) Comparison of recorded (gray line), simulated (thick black line) and optimal (thin black line) muscle activity in several extensor muscles crossing the knee and ankle joints. VAF of the data-matched simulations (TSyID) for muscles shown ranged from 85–91%. VAF of the simulations from the optimal DQR prediction for the muscle shown ranged from 84–90%.

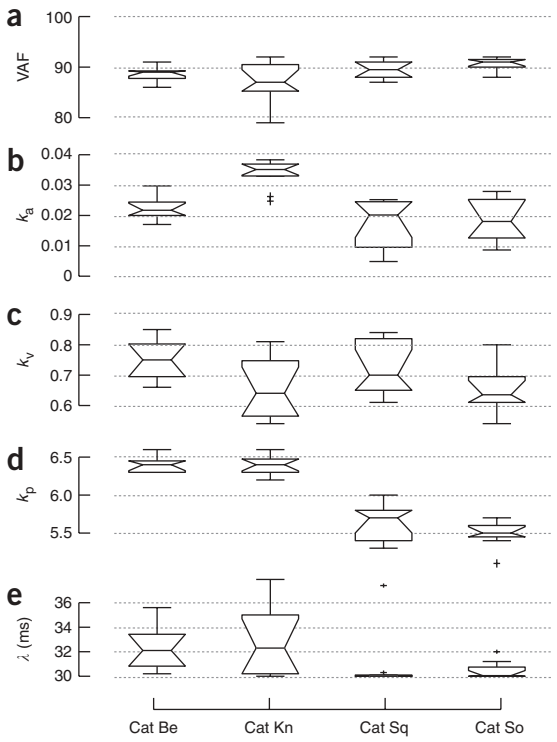

Figure 4 Summary of model (TSyID) fits and parameter values (mean ± s.d.) for all muscles in four cats. (**a**) VAF was greater than 80% in all muscles in each cat. (**b**) Acceleration feedback gain, k_a, for all muscles in each cat. (**c**) Velocity feedback gain, k_v, for all muscles in each cat. (**d**) Position feedback gain, k_p, for all muscles in each cat. These results demonstrate that similar feedback gains are used across all muscles in each animal, suggesting that they are activated by a common neural command signal. (**e**) Delay, λ, for all muscles in each cat. For cats Be, Kn, Sq and So, 9, 7, 10 and 8 left hindlimb muscles were analyzed, respectively. In cat Kn, 4 left forelimb muscles were also included.

of the muscles. To our surprise, the antagonistic, flexor muscle responses in both cases (**Fig. 5c,d**) were similar to those predicted by the model (**Fig. 5c**).

Optimal control model of posture

We compared the neural feedback gains identified through TSyID with an optimal solution predicted without a priori knowledge of the experimental CoM kinematics or muscle activations. We used an optimal control formulation that was similar to the linear quadratic regulator formulation devised previously in postural control models[27]. We dubbed our approach a delayed quadratic regulator (DQR) because it incorporated a time delay and determined optimal feedback gains via a quadratic cost function. In contrast with other models[28–30], we used experimentally measured platform acceleration to generate perturbations with realistic temporal characteristics. The delay was set to the value estimated through TSyID ($\sim$30 ms), thus representing a constraint of the neural transmission and computation time, as the optimal delay would be a nonphysiological value of zero.

The optimal solution predicted a postural response with initial burst and plateau regions that were similar to those measured experimentally (for example, **Fig. 3d**; VAF = 78 ± 6% s.e.m., across all muscles in all cats, VAF > 70% in all muscles) and were also similar to those estimated through TSyID (**Fig. 3d**). Using measured perturbation acceleration was critical for achieving a physiologically relevant muscle-activation pattern because of the dependence of the sensory feedback on the exact perturbation characteristics.

Changes following sensory loss

We observed notable changes in temporal patterns of muscle activation in animals with large-fiber (group I) proprioceptive deficit as a result of pyridoxine overdose. Proprioceptive afferents are critical for generating the proper timing in postural responses; postural responses are delayed following proprioceptive loss but not following vestibular or visual loss[17,31–33]. The pyridoxine intoxication affected sensory afferent fibers larger than 10 μm in diameter, including primary muscle spindle afferents, Golgi tendon organ afferents and large cutaneous afferents[17]. In the days following the pyridoxine injections, the loss of group I afferents was devastating; animals became ataxic, and in many cases lost the ability to stand independently. Over a period of about 2 weeks, animals regained the ability to stand and be mobile, although group I afferents remained nonfunctional, as determined by stretch-reflex tests and histological measurements[17]. Sensory-deficit animals could stand and maintain their balance, presumably using smaller group II afferents. We analyzed postural responses after a $\sim$3-week period of re-adaptation, when animals had recovered postural control and other motor functions.

In the animal with the greatest sensory deficit, the initial burst (**Fig. 3**) of the temporal muscle-activation pattern was absent (**Fig. 6**). Instead, muscle activity was characterized by a long, slow rise in muscle activation. These changes were previously described simply as an increase in response latency and amplitude[17].

Changes in temporal patterns of muscle activation following large-fiber sensory loss were due to decreased CoM-acceleration feedback. A 50% reduction of the acceleration feedback gain accounted for the diminished initial peak in animals with the complete loss of afferents in the group I (<10-μm diameter; cat Be and cat Kn) range (**Table 1**). In these animals, fits were improved when the acceleration feedback was explicitly set to zero (ΔVAF = +2%, $P < 0.01$). In animals with only a partial loss of group I afferents (**Table 1**), acceleration bursts were still present, and fits were degraded when acceleration feedback was set to zero (ΔVAF = –3%, $P < 0.01$). Although the quantitative effects of removing acceleration were modest because the acceleration component contributes only a small amount to the overall temporal variance of the signal, the qualitative loss of the initial burst was very noticeable.

The optimal muscle-activation pattern predicted by the DQR model in the absence of acceleration feedback was notably similar to what was actually measured (for example, **Fig. 6e**; VAF = 65 ± 6%). The resulting optimal pattern was characterized by a slow rise in muscle activation, which was expected as a result of the loss of acceleration feedback. An increase in velocity gain was predicted to compensate for the loss of the initial burst (5% increase, $P \ll 0.01$). The optimal prediction has only slightly decreased postural stability compared with the intact condition and produced qualitatively similar CoM velocity and displacement trajectories (**Figs. 3a** and **6a**).

Therefore, after the recovery of balance control in sensory-impaired animals, the extrinsic, task-level variables of CoM position and velocity are still regulated, albeit with different sensory pathways. Redundancy and neural plasticity mechanisms presumably upregulate the contribution of group II sensory signals in the regulation of postural control. Thus, the new temporal patterns of muscle activation that the animal achieves after a period of re-adaptation reflect a process of optimal reweighting of sensory feedback to maintain control of extrinsic, task-level variables.

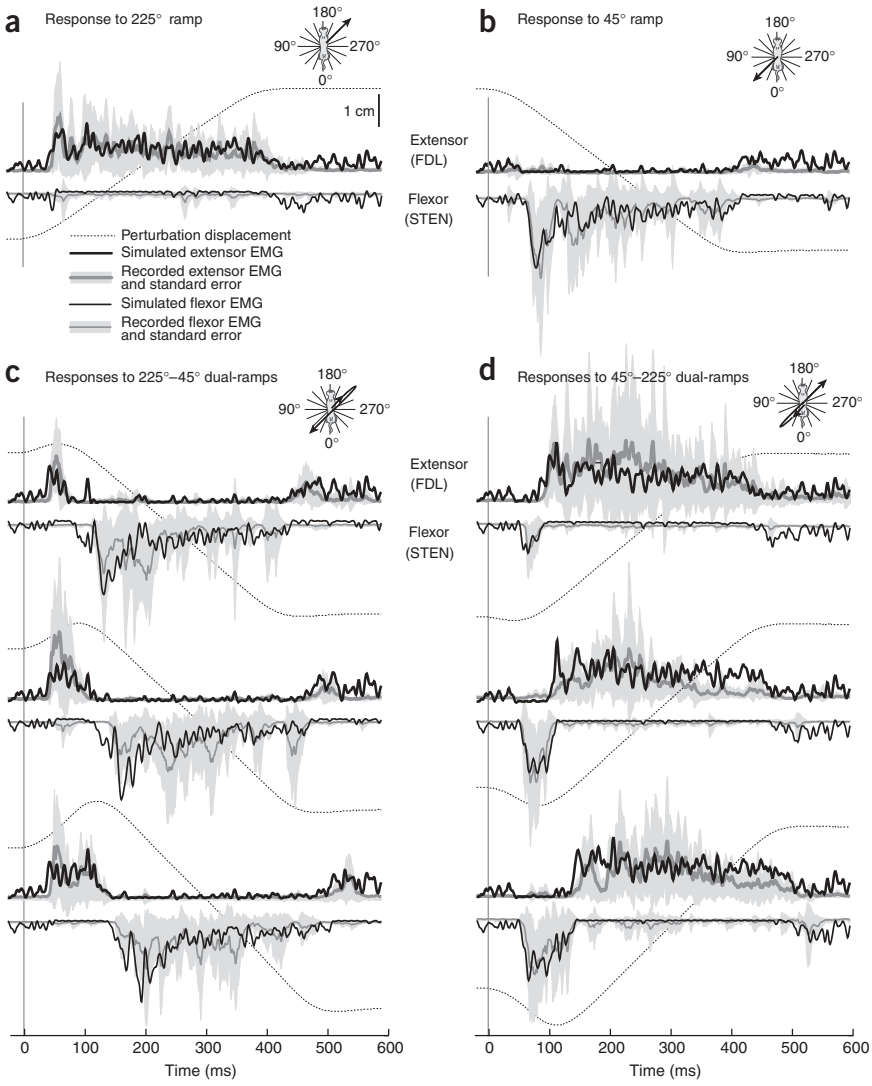

Figure 5 Robustness of the feedback model to varying perturbation characteristics. We predicted responses to dual-ramp perturbations using the feedback gains derived from responses to ramp-and-hold perturbations in an extensor and flexor muscle. (**a**) Extensor response to a 225° ramp-and-hold perturbation (thick gray lines) and simulated TSyID response (thick black lines). (**b**) Flexor response to a 45° ramp-and-hold perturbation (thin gray lines) and simulated TSyID response (thin black lines). (**c**) Responses to 225°–45° ramp-and-hold perturbations (dashed black lines) with varying initial ramp duration. The extensor muscle (thick gray lines) was initially activated and rapidly shut down as the perturbation reversed direction, activating the flexor muscles (thin gray lines). Over all of the perturbations, the muscle activity is predicted by the model using a fixed set of feedback gains derived from the perturbations shown in **a** and **b**. The model predicted the switching between the extensor (thick black lines) and flexors (thin black lines), as well as the changes in the short initial burst of the extensor muscles. The timing of the extensor burst at the termination of the secondary ramp is also predicted. (**d**) Response to a 45°–225° dual-ramp perturbation. The initial flexor burst is well-predicted, as is the timing and amplitude of the longer extensor burst. Overall, the changes in muscle activity can be characterized by a common set of feedback gains and are therefore due to differences in perturbation characteristics processed through a common sensorimotor transformation.

DISCUSSION

We demonstrated that neural commands to multiple muscles are modulated by extrinsic, task-level movement parameters through a low-dimensional feedback transformation. The sensorimotor transformation for balance control is a delayed-feedback rule using CoM kinematics, which are dynamically affected by both the perturbation and the ongoing motor response. The time courses of multiple muscle-activation patterns throughout the postural response are dependent on information from multiple sensory receptors, which can be re-weighted when specific populations of sensory afferents are damaged following large-fiber sensory neuropathy. The postneuropathy feedback transformation takes advantage of the available sensory information in redundant sensory afferents.

We present quantitative evidence demonstrating that a hierarchal neural feedback controller modulates muscle synergies in vertebrate motor systems. Prior studies have suggested that a similar, linear neural control mechanism might sit at the top of a complex hierarchy of sensorimotor feedback loops used for voluntary-movement control[12,14,15]. Our results explicitly demonstrate a low-dimensional hierarchal control structure in a natural and biomechanically unstable multijoint task that does not require trajectory planning[10]. Temporal activity in multiple muscles crossing multiple joints reflects the dynamic changes in the task-level variables that are being controlled. The temporal pattern reflects a weighted sum of the acceleration, velocity and position of the task variable, similar to the temporal patterning of neural population vectors in the motor cortex during reaching movements[12,13,34]. The command signals, based on task-variable feedback, are distributed spatially to multiple muscles across the body[5], consistent with the muscle-synergy hypothesis, whereby a single neural command activates multiple muscles with specific relative patterns of activation[1–4]. In our scheme, each feedback gain can activate a different muscle-synergy pattern, allowing flexibility in the spatiotemporal coordination of multiple muscles[5].

Although the exact neural mechanisms regulating postural control are unknown, evidence suggests that the hierarchal controller for posture resides in supraspinal circuits, possibly in the brainstem. Classic experiments have demonstrated that decerebrated cats are able to produce righting responses and walk[35]. In contrast, animals with complete spinal cord transection can walk, but do not produce directionally specific postural responses[36], and supraspinal connections to the spinal cord are essential for maintaining postural orientation[35]. Because postural responses are essentially absent following spinal cord transection, and the cerebral cortex is not required for postural orientation, we propose that the brainstem is critical for the estimation of task-level variables for directional postural control in response to disturbances. However, whether muscle synergies themselves are encoded in the brainstem or in the spinal cord is still an open question. Regardless, the roles of spinal circuits[37] and musculoskeletal properties[38] in facilitating interjoint stability and coordination are critical to

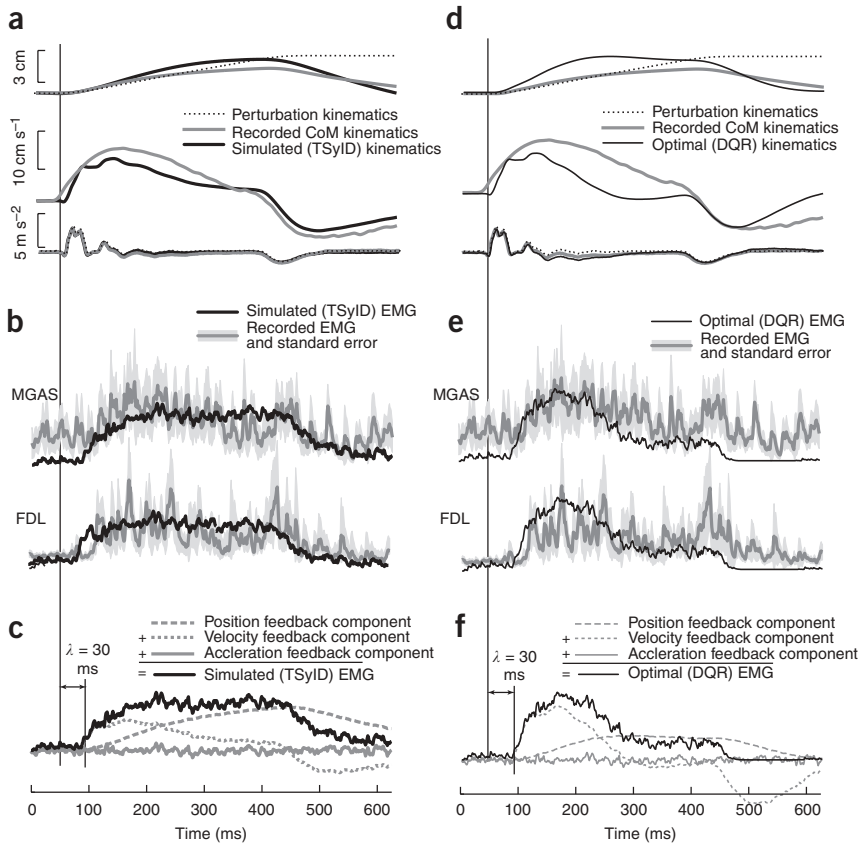

Figure 6 Comparison of recorded and simulated muscle activation and CoM kinematics following large-fiber neuropathy. (**a**) Recorded (gray lines) and simulated CoM kinematics (thick black lines) using parameters from TSyID. (**b**) Recorded muscle activity (gray lines) in the MGAS and FDL, and simulated muscle activity (thick black lines) from the best-match model parameters derived from the TSyID formulation of the model (VAF = 87 and 90%, respectively). (**c**) Decomposition of simulated muscle activity (black line) into components arising from CoM position feedback (gray dashed line), CoM velocity feedback (gray dotted line) and CoM acceleration feedback (gray solid line). Note that acceleration feedback is absent. (**d**) Recorded (gray lines) and simulated CoM kinematics (thick black lines) from optimal DQR formulation. (**e**) Recorded muscle activity (gray lines) in the MGAS and FDL and simulated muscle activity (thick black lines) from optimal DQR formulation of the model (VAF = 77 and 83%, respectively). (**f**) Decomposition of simulated muscle activity (black line) into components arising from CoM position feedback (gray dashed line), CoM velocity feedback (gray dotted line) and CoM acceleration feedback (gray solid line). Note that acceleration feedback (gray solid line) is absent.

the implementation of a low-dimensional, hierarchal controller and warrant further study[15,39].

The computation of task-level variables requires substantial multisensory integration. Particularly in postural control, local variables arising from visual, vestibular and various proprioceptive afferents are each insufficient to account for body orientation and multisegmental coordination. Local feedback of sensory signals cannot explain postural behaviors in humans or cats, particularly in situations of sensory conflict where an erroneous sensory signal must be ignored[5,29,40,41]. We demonstrate that the CoM kinematic signals are the relevant task-level variables that encapsulate the relationship between the body and the extrinsic reference frame and define the temporal patterns of muscle activation used in postural control. But CoM motion cannot be reliably derived from any single sensory afferent population[9,10,40]. As this study does not address how the task-level variables are computed from local, anatomical variables, further study and validation of more complex models[28] that explicitly include redundant sensor and muscle dynamics is warranted.

Our model defines a framework for understanding functional feedback gains that are specified at a hierarchal control level, but whose specific implementation at a local, anatomical level may vary as a result of sensory and motor redundancy[5]. Our data demonstrate that, after a period of re-adaptation, the task-level feedback hierarchy for balance control was maintained when specific local sensory afferent pathways were eliminated. Loss of group I afferents produced short-term ataxia and an inability to maintain standing balance control. But after a period of re-adaptation, the nervous system was able to adequately estimate CoM position and velocity, but not acceleration, for postural control. Presumably, contributions of sensory information from group II afferents used to estimate CoM motion were increased by the nervous system to make up for the loss of group I information. Similarly, reweighting of position and velocity information from different sensory modalities explains changes in body motion when visual or vestibular information is absent[29,30]. The surprising robustness of our simple feedback model suggests that manipulating the strength of local sensory-feedback pathways to maintain hierarchal, functional feedback gains regulating task-level variables is a fundamental strategy of the nervous system for dealing with changing sensory conditions.

Hierarchal and functional feedback gains may be flexibly modulated by descending neural commands to modify postural responses under different conditions[5]. Animals were able to compensate well for the loss of CoM acceleration information and were able to regulate their balance with only small differences in CoM kinematics from the intact condition. This illustrates nicely the redundancy in temporal muscle-activation patterns; acceleration feedback is not biomechanically necessary for adequate balance control but reflects a preferred neural transformation for balance control in the intact condition. Our animals

Table 1 Grand mean feedback gains and delay before and after sensory loss

	%VAF	k_p	k_v	k_a	λ
Cat Be intact	89 ± 2	5.7 ± 0.1	0.75 ± 0.06	0.022 ± 0.004	32 ± 2
Sensory loss#	88 ± 3	5.4 ± 0.2**	0.69 ± 0.07*	0.011 ± 0.009**	30 ± 1
Cat Kn Intact	87 ± 4	6.4 ± 0.1	0.65 ± 0.10	0.034 ± 0.004	34 ± 5
Sensory loss#	88 ± 7	5.9 ± 0.1*	0.68 ± 0.06	0.016 ± 0.007**	30 ± 1
Cat Sq Intact	89 ± 2	5.6 ± 0.2	0.72 ± 0.08	0.018 ± 0.008	31 ± 2
Sensory loss&	88 ± 2	6.2 ± 0.2**	0.64 ± 0.09**	0.027 ± 0.007**	40 ± 6
Cat So intact	91 ± 1	5.5 ± 0.2	0.65 ± 0.08	0.019 ± 0.080	30 ± 1
Sensory loss&	85 ± 2	5.4 ± 0.2	0.75 ± 0.75**	0.019 ± 0.007	32 ± 3

#complete sensory loss in group I range; for example, no afferents >10-μm diameter. &partial sensory loss in group I range; for example, some afferents >10-μm diameter. *sensory loss condition is significantly different from the intact condition at $P < 0.05$ level. **sensory loss condition is significantly different from the intact condition at the $P < 0.01$ level.

were trained long-term on the postural perturbation procedure and their responses were comparable to an optimal solution. However, under different conditions, the desired tradeoff between neural effort and biomechanical stabilization may vary, altering the optimal feedback-gain values. The latencies and spatiotemporal patterns of response in naive animals are similar to trained animals, but the amplitude and duration are increased[40]. With experience, greater motion of the CoM may be tolerated in return for lower energy expenditure and neural effort. We predict that variations in postural responses as a result of cognitive and emotional influences, or prior experience[10,42], may be explained by variations in the strength of hierarchal feedback gains.

Our findings demonstrate that the nervous system uses acceleration information for generating motor commands; further investigation into the nature of acceleration encoding is warranted. Acceleration feedback is lost following sensory loss in the group I range, implicating muscle spindles, Golgi tendon organs and cutaneous receptors in the encoding of acceleration. As early as the 1950s, it has been postulated that muscle spindles can encode acceleration[43,44]. It is also possible that the acceleration information is encoded in the Golgi tendon organs, as forces in an active muscle may vary in relation to acceleration. The contributions of cutaneous receptors, which can respond dynamically to pressure on the skin[45], cannot be ruled out either. Although acceleration feedback is responsible for the fast initial rise in muscle activation, our results are consistent with previous findings that velocity feedback accounts for the bulk of the functional response[46] (**Fig. 3c**).

The simple neural transformation identified here, and its adaptation following sensory loss, may reflect general neuromotor control strategies and warrants further investigation. Many muscles are activated by weighted combinations of the same temporal patterns, which is consistent with a reduced dimension descending control structure for extrinsic, task-level variables using muscle synergies[4,13,15,47,48]. Similarly, muscle synergies may arise naturally in optimal motor behaviors[48]. The recognition that task-level, and not anatomical, variables are regulated in balance control could help to identify neural circuits that underlie balance control. Moreover, it is likely that a similar transformation occurs in other types of motor responses where the nervous system must alter a motor output in response to a perturbation, as in fingertip grip response[45], or in responses to perturbations during reaching[49]. Finally, the comparison of experimentally measured responses to different optimal control solutions may help test hypotheses regarding the nature of neuromotor adaptation.

METHODS

Data collection. We collected data from postural perturbations in the standing cat. Detailed experimental and training procedures have been described previously[18]. Three cats (of mean mass 3.8 kg) were trained to stand freely with each foot on a force plate. Muscle activity from chronic indwelling electrodes was recorded from a subset of 8–15 left hindlimb muscles in each of four cats; in one animal (cat Kn), four forelimb muscles were also recorded.

Two types of perturbations were applied along a diagonal axis to elicit maximal extensor and flexor activity in the left hindlimb, and to minimize the contributions of the other three limbs[18]. Left hindlimb extensor muscles were maximally activated when the platform translated forward and to the right[18] (**Fig. 1a**). The first type of perturbation was a single ramp-and-hold translation in the forward-right direction (225°) of 5-cm amplitude, 370-ms duration and 15-cm s^{-1} mean velocity. The second type of perturbation was a dual ramp that began movement in the forward-right direction, but then reversed direction after a variable duration of 20–90 ms. This altered the initial acceleration of the platform and elicited a short response of the extensor muscles, followed by a response in flexor muscles (**Fig. 1b**).

We collected postural responses in the same cats following peripheral neuropathy that was induced by pyridoxine (vitamin B6) intoxication[17]. Pyridoxine overdose initiates sensory loss in the peripheral and central processes of myelinated primary afferent fibers in humans, dogs, rats and cats; our doses were designed to induce deficits only in the group I range (10–20 μm)[17].

Five trials of each perturbation type were collected per day. We analyzed data from 3 different days in intact animals. After pyridoxine intoxication, we analyzed the last day of data collection, when animals had recovered the ability to stand on the platform. Position and acceleration of the support surface, ground reaction forces and electromyograms (EMGs) were collected at 1,000 Hz. Forces were low-pass filtered at 100 Hz, and raw EMG data were high-pass filtered at 35 Hz, demeaned, rectified and low-pass filtered at 40 Hz. CoM kinematics of the cat were computed by integrating the summed ground reaction forces. Average kinematic, kinetic and EMG data for each condition were computed for each day of data collection.

Feedback control model. A model of an inverted pendulum on a cart was used to represent the overall dynamics of the standing cat. The neural controller was modeled as a linear feedback loop with a lumped time delay. Using this model, we used two optimization techniques to determine the appropriate feedback gains and delay: (i) a TSyID technique in which temporal EMG and kinematic responses were used in a tracking optimization and (ii) a data-independent optimal solution using a quadratic cost function, referred to as a DQR.

The inverted pendulum reasonably approximated the dynamics of the cat, as the limb axis rotates about the toe joint like an inverted pendulum and joint angle changes are $\leq 6°$ (ref. 9). The linearized equation of motion for the pendulum is:

$$\ddot{\theta} = \frac{g}{l}\theta + \frac{T}{ml^2}$$

where θ is the angle of the pendulum with respect to the vertical, m and l are the mass and height of the CoM of the cat, respectively, and T is the applied torque at the pin joint. A mass of 4 kg and a height of 20 cm were used.

Because the actual platform kinematics were not identical to the specified kinematics, and because the exact perturbation characteristic were critical to the predicted EMG signals, we applied recorded platform-acceleration data to the model. Support-surface perturbations were modeled by converting measured linear platform acceleration into a disturbance torque about the base of the pendulum and linearizing:

$$T_{\text{pert}} = ml \cdot a(t)$$

where T is disturbance torque, and $a(t)$ is the measured linear acceleration of the support surface.

The neural controller was modeled as three feedback channels on the horizontal position, velocity and acceleration of the pendulum and the lumped time-delay at the input to the feedback loop. Because neural latencies exist between the onset of a perturbation and the onset of the EMG response (30–60 ms), this delay could not be ignored when predicting temporal EMG patterns. The control effort of our system u, which is equivalent to the predicted EMG signal, was a linear combination of time-delayed horizontal CoM position (x), velocity ($\dot{x}$) and acceleration ($\ddot{x}$):

$$u(t) = k_a\ddot{x}(t-\lambda) + k_v\dot{x}(t-\lambda) + k_p x(t-\lambda)$$

where t is time, λ is a time delay, and k_p, k_v and k_a are feedback gains for position, velocity and acceleration, respectively. The three feedback gain values and time delay were chosen via optimization methods. The predicted EMG, u, was transformed to torque on the pin joint of the pendulum using a first-order muscle model with a time constant of 40 ms[27].

TSyID. System identification in the time domain was carried out to determine values for the three feedback gains and time delay using a tracking optimization that minimized the error between recorded and predicted EMG and CoM kinematics. A cost index, J, was defined to be a linear combination of the square of error terms, and the maximum of the square of error terms:

$$\min_{k_p,k_v,k_a,\lambda}\left[J = \int_0^T \left(\sum_i e_i^T \mu_i e_i + \max \sum_i \mu_i e_i^2\right)dt\right]$$

where e_m, e_p, e_v and e_a are the differences between recorded and predicted EMG, and CoM position, velocity and acceleration, respectively, and μ_m, μ_p, μ_v and μ_a

are weighting coefficients used for normalizing across units (set to 1.0, 0.01, 0.02 and 1.0, respectively). A set of admissible gains was defined by extending a liberal window around the nominal region of convergence.

Optimal parameter values quantified by J were found using a MATLAB (Mathworks) optimization package (*fmincon.m*). White Gaussian noise with a mean of zero was injected into each feedback channel[30,50]. This noise caused gradient-descent optimization methods to converge to a more repeatable solution. Variances for the noise in the feedback channels were set to be $\sigma_p = 0.0001$ m, $\sigma_v = 0.001$ m s^{-1} and $\sigma_a = 0.01$ m s^{-2}.

DQR optimization. In addition to the TSyID optimization, a quadratic cost index was used to predict EMG and CoM kinematics a priori, that is, without reference to the recorded data. The quadratic cost index penalized deviations from zero of the pendulum position, velocity and acceleration, the predicted EMG and the final position of the pendulum:

$$\min_{k_p,k_v,k_a}\left[J = \int_0^T (x^T Q x + \rho u^2)dt + \Omega \cdot x(T)\right]$$

where $Q = diag(q_p q_p q_p)$ is the weighting for CoM kinematic deviation, ρ is a weighting on predicted EMG and Ω is a weighting vector for the terminal state values. The same weightings were used as in the TSyID formulations. Because optimization always pushes the time delay to the minimum allowable value, the delay length was set to be equal to the value found in the TSyID method. Thus, the DQR optimization only incorporated the three feedback gains that were found using a MATLAB optimization package (*fmincon.m*).

ACKNOWLEDGMENTS

We thank J.M. Macpherson and P.J. Stapley for use of the data and helpful comments, R.J. Peterka for his technical guidance, A. Koenig for help with the simulations, and J.L. McKay for his insightful editorial assistance. This work was supported by Whitaker Grant RG–02–0747.

AUTHOR CONTRIBUTIONS

D.B.L. developed and validated the TSyID and DQR formulations, performed the simulations and data analysis and contributed to writing the manuscript. L.H.T. conceptualized the model, developed the dual-ramp perturbations, participated in experiments, supervised the research and wrote the manuscript.

Published online at http://www.nature.com/natureneuroscience
Reprints and permissions information is available online at http://npg.nature.com/reprintsandpermissions

1. Tresch, M.C., Saltiel, P. & Bizzi, E. The construction of movement by the spinal cord. *Nat. Neurosci.* **2**, 162–167 (1999).
2. Ting, L.H. & Macpherson, J.M. A limited set of muscle synergies for force control during a postural task. *J. Neurophysiol.* **93**, 609–613 (2005).
3. d'Avella, A. & Bizzi, E. Shared and specific muscle synergies in natural motor behaviors. *Proc. Natl. Acad. Sci. USA* **102**, 3076–3081 (2005).
4. Flash, T. & Hochner, B. Motor primitives in vertebrates and invertebrates. *Curr. Opin. Neurobiol.* **15**, 660–666 (2005).
5. Ting, L.H. Dimensional reduction in sensorimotor systems: a framework for understanding muscle coordination of posture. in *Computational Neuroscience: Theoretical Insights into Brain Function, Progress in Brain Research* **165** (eds. Cisek, P., Drew, T. & Kalaska, J.F.) 301–325 (Elsevier, Amsterdam, 2007).
6. Cappellini, G., Ivanenko, Y.P., Poppele, R.E. & Lacquaniti, F. Motor patterns in human walking and running. *J. Neurophysiol.* **95**, 3426–3437 (2006).
7. d'Avella, A., Saltiel, P. & Bizzi, E. Combinations of muscle synergies in the construction of a natural motor behavior. *Nat. Neurosci.* **6**, 300–308 (2003).
8. Poppele, R. & Bosco, G. Sophisticated spinal contributions to motor control. *Trends Neurosci.* **26**, 269–276 (2003).
9. Ting, L.H. & Macpherson, J.M. Ratio of shear to load ground-reaction force may underlie the directional tuning of the automatic postural response to rotation and translation. *J. Neurophysiol.* **92**, 808–823 (2004).
10. Horak, F.B. & Macpherson, J.M. Postural orientation and equilibrium. in *Handbook of Physiology, Section 12*, 255–92 (American Physiological Society, New York, 1996).
11. Gollhofer, A., Horstmann, G.A., Berger, W. & Dietz, V. Compensation of translational and rotational perturbations in human posture: stabilization of the centre of gravity. *Neurosci. Lett.* **105**, 73–78 (1989).
12. Todorov, E. Direct cortical control of muscle activation in voluntary arm movements: a model. *Nat. Neurosci.* **3**, 391–398 (2000).
13. Graziano, M. The organization of behavioral repertoire in motor cortex. *Annu. Rev. Neurosci.* **29**, 105–134 (2006).
14. Scott, S.H. Optimal feedback control and the neural basis of volitional motor control. *Nat. Rev. Neurosci.* **5**, 532–546 (2004).
15. Todorov, E., Li, W. & Pan, X. From task parameters to motor synergies: a hierarchical framework for approximately optimal control of redundant manipulators. *J. Robot Syst.* **22**, 691–710 (2005).
16. Loeb, G.E., Brown, I.E. & Cheng, E.J. A hierarchical foundation for models of sensorimotor control. *Exp. Brain Res.* **126**, 1–18 (1999).
17. Stapley, P.J., Ting, L.H., Hulliger, M. & Macpherson, J.M. Automatic postural responses are delayed by pyridoxine-induced somatosensory loss. *J. Neurosci.* **22**, 5803–5807 (2002).
18. Macpherson, J.M. Strategies that simplify the control of quadrupedal stance. II. Electromyographic activity. *J. Neurophysiol.* **60**, 218–231 (1988).
19. Diener, H.C., Horak, F.B. & Nashner, L.M. Influence of stimulus parameters on human postural responses. *J. Neurophysiol.* **59**, 1888–1905 (1988).
20. Bosco, G., Poppele, R.E. & Eian, J. Reference frames for spinal proprioception: limb endpoint based or joint-level based? *J. Neurophysiol.* **83**, 2931–2945 (2000).
21. Nashner, L.M. Adapting reflexes controlling the human posture. *Exp. Brain Res.* **26**, 59–72 (1976).
22. Risher, D.W., Schutte, L.M. & Runge, C.F. The use of inverse dynamics solutions in direct dynamics simulations. *J. Biomech. Eng.* **119**, 417–422 (1997).
23. Torres-Oviedo, G., Macpherson, J.M. & Ting, L.H. Muscle synergy organization is robust across a variety of postural perturbations. *J. Neurophysiol.* **96**, 1530–1546 (2006).
24. Torres-Oviedo, G. & Ting, L.H. Muscle synergies characterizing human postural responses. *J. Neurophysiol.* published online 25 July 2007 (doi:10.1152/jn.01360.2006).
25. Alexandrov, A.V., Frolov, A.A. & Massion, J. Biomechanical analysis of movement strategies in human forward trunk bending. I. Modeling. *Biol. Cybern.* **84**, 425–434 (2001).
26. van Antwerp, K.W., Burkholder, T.J. & Ting, L.H. Interjoint coupling effects on muscle contributions to endpoint force and acceleration in a musculoskeletal model of the cat hindlimb. *J. Biomech.* published online 17 July 2007 (doi:10.1016/j.jbiomech.2007.06.001).
27. He, J.P., Levine, W.S. & Loeb, G.E. Feedback gains for correcting small perturbations to standing posture. *Proceedings of the 28th IEEE Conference on Decision and Control, 1989.* **1**, 518–526 (1991).
28. Jo, S. & Massaquoi, S.G. A model of cerebellum stabilized and scheduled hybrid long-loop control of upright balance. *Biol. Cybern.* **91**, 188–202 (2004).
29. Kuo, A.D. An optimal state estimation model of sensory integration in human postural balance. *J. Neural Eng.* **2**, S235–S249 (2005).
30. Peterka, R.J. Sensorimotor integration in human postural control. *J. Neurophysiol.* **88**, 1097–1118 (2002).
31. Inglis, J.T., Horak, F.B., Shupert, C.L. & Jones-Rycewicz, C. The importance of somatosensory information in triggering and scaling automatic postural responses in humans. *Exp. Brain Res.* **101**, 159–164 (1994).
32. Inglis, J.T. & Macpherson, J.M. Bilateral labyrinthectomy in the cat: effects on the postural response to translation. *J. Neurophysiol.* **73**, 1181–1191 (1995).
33. Runge, C.F., Shupert, C.L., Horak, F.B. & Zajac, F.E. Role of vestibular information in initiation of rapid postural responses. *Exp. Brain Res.* **122**, 403–412 (1998).
34. Georgopoulos, A.P., Schwartz, A.B. & Kettner, R.E. Neuronal population coding of movement direction. *Science* **233**, 1416–1419 (1986).
35. Deliagina, T.G., Zelenin, P.V., Beloozerova, I.N. & Orlovsky, G.N. Nervous mechanisms controlling body posture. *Physiol. Behav.* published online 21 May 2007 (doi:10.1016/j.physbeh.2007.05.023).
36. Macpherson, J.M. & Fung, J. Weight support and balance during perturbed stance in the chronic spinal cat. *J. Neurophysiol.* **82**, 3066–3081 (1999).
37. Hyngstrom, A.S., Johnson, M.D., Miller, J.F. & Heckman, C.J. Intrinsic electrical properties of spinal motoneurons vary with joint angle. *Nat. Neurosci.* **10**, 363–369 (2007).
38. Lin, D.C. & Rymer, W.Z. Damping actions of the neuromuscular system with inertial loads: soleus muscle of the decerebrate cat. *J. Neurophysiol.* **83**, 652–658 (2000).
39. Todorov, E. Optimality principles in sensorimotor control. *Nat. Neurosci.* **7**, 907–915 (2004).
40. Nashner, L.M. Fixed patterns of rapid postural responses among leg muscles during stance. *Exp. Brain Res.* **30**, 13–24 (1977).
41. Macpherson, J.M., Everaert, D.G., Stapley, P.J. & Ting, L.H. Bilateral vestibular loss in cats leads to active destabilization of balance during pitch and roll rotations of the support surface. *J. Neurophysiol.* **97**, 4357–4367 (2007).
42. Macpherson, J.M. The force constraint strategy for stance is independent of prior experience. *Exp. Brain Res.* **101**, 397–405 (1994).
43. Schafer, S.S. The acceleration response of a primary muscle-spindle ending to ramp stretch of the extrafusal muscle. *Experientia* **23**, 1026–1027 (1967).
44. Boyd, I.A. The histological structure of the receptors in the knee joint of the cat correlated with their physiologic response. *J. Physiol. (Lond.)* **124**, 476–488 (1954).
45. Johansson, R.S., Riso, R., Hager, C. & Backstrom, L. Somatosensory control of precision grip during unpredictable pulling loads. I. Changes in load force amplitude. *Exp. Brain Res.* **89**, 181–191 (1992).
46. Jeka, J., Kiemel, T., Creath, R., Horak, F.B. & Peterka, R.J. Controlling human upright posture: velocity information is more accurate than position or acceleration. *J. Neurophysiol.* **92**, 2368–2379 (2004).
47. Poggio, T. & Bizzi, E. Generalization in vision and motor control. *Nature* **431**, 768–774 (2004).
48. Chhabra, M. & Jacobs, R.A. Properties of synergies arising from a theory of optimal motor behavior. *Neural Comput.* **18**, 2320–2342 (2006).
49. Soechting, J.F. & Lacquaniti, F. Quantitative evaluation of the electromyographic responses to multidirectional load perturbations of the human arm. *J. Neurophysiol.* **59**, 1296–1313 (1988).
50. van der Kooij, H., Jacobs, R., Koopman, B. & Grootenboer, H. A multisensory integration model of human stance control. *Biol. Cybern.* **80**, 299–308 (1999).